J Mater Sci (2007) 42:87–92
DOI 10.1007/s10853-006-1044-1

PMMA nanocomposites and gradient materials prepared by means of polysilsesquioxane (POSS) self-assembly

Hans Weickmann · Ralf Delto · Ralf Thomann · Rüdiger Brenn · Walter Döll · Rolf Mülhaupt

Received: 18 October 2005 / Accepted: 10 January 2006 / Published online: 18 November 2006

Abstract PMMA nanocomposites were prepared by means of self-assembly of polyhedral oligomeric silsesquioxanes (POSS) such as $[Si_8O_{12}(OSiMe_2H)_8]$ (POSS1) and $[Si_7O_9(cyclohexyl)_7(OSiMe_2H)_3]$ (POSS2) during the free radical methyl methacrylate (MMA) bulk polymerization. The POSS phases separation and self-assembly afforded in situ nanocubes with average diameters ranging from 25 nm to 500 nm. The influence of 5.3 wt.% POSS on the thermal, mechanical and morphological PMMA nanocomposite properties was investigated. POSS mediated nanocube formation was accompanied by improvements of PMMA glass temperature and toughness. Depth profiling by means of ion beam Rutherford backscattering (RBS) analysis indicated the accumulation of POSS1 at the PMMA surface.

Introduction

The dispersion of nanometer-scaled fillers within a polymer matrix represents an attractive route to prepare polymer nanocomposites. In contrast to conventional micro-fillers most of the polymer in nanocomposites is located at the nanofiller interfaces. The conversion of bulk polymers into interfacial polymers offers new opportunities to tailor polymer property profiles. Very low filler contents of a few weight percent can be sufficient to improve stiffness, strength and dimensional stability simultaneously without sacrificing toughness, to enhance barrier resistance and to improve thermal stability as well as halogen-free flame retardency [1–5]. During the last decade polyhedral oligomeric silsesquioxanes (POSS) have attracted considerable attention as molecular silica and nanometer-scaled building blocks for the nanocomposite formation [6–13]. The term silsesquioxane denotes organic compounds of the general formula $[RSiO_{3/2}]_{n\geq 4}$. The silsesquioxanes exhibit a wide variety of different molecular architectures ranging from random-coil and rigid polymers to well-defined small molecular weight molecules [14]. The Si_8O_{12} POSS family exhibits cage-like architectures and nanometer-scale dimensions of approximately 15 Å (Scheme 1). Today POSS is readily available and can be functionalized with various functional groups such as e.g., epoxy [6, 7], styryl [8], methacryloyl [9, 10], vinyl [11, 12] and hydrido [12, 13] in order to achieve copolymerization, crosslinking and interfacial coupling.

Numerous groups use fine-tuned POSS molecular architectures in order to prepare nanocomposites by means of POSS copolymerization. For example, Zheng et al. attached monofunctional vinylbenzene functionalized POSS to the polystyrene backbone by means of free radical copolymerization with styrene [11]. Improved thermal stability as well as higher degradation temperatures were reported. Similar results were

H. Weickmann · R. Thomann · R. Mülhaupt (✉)
Institut für Makromolekulare Chemie and Freiburger Materialforschungszentrum der Albert-Ludwigs-Universität, Stefan-Maier-Str. 31, D-79104 Freiburg i. Br., Germany
e-mail: rolf.muelhaupt@makro.uni-freiburg.de

R. Delto · R. Brenn
Physikalisches Institut der Albert-Ludwigs-Universität, Hermann-Herder-Str. 3, D-79104 Freiburg i. Br., Germany

W. Döll
Fraunhofer Institut für Werkstoffmechanik, Wöhlerstr. 11, D-79108 Freiburg i. Br., Germany

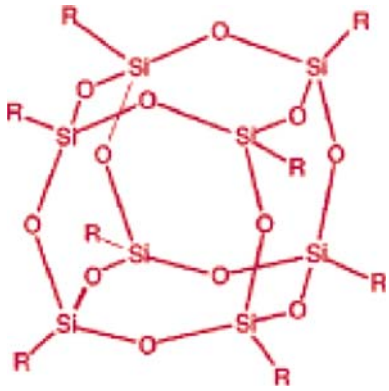

Scheme 1 Polyhedral oligomeric silsesquioxanes (POSS)

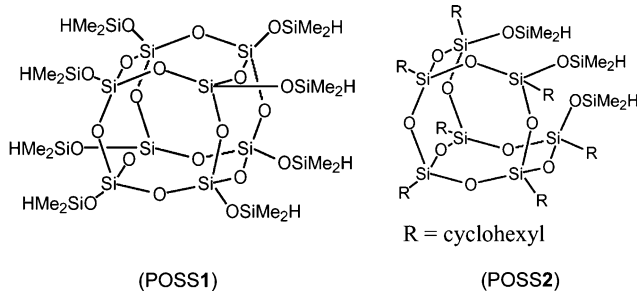

Scheme 2 Structure of OctaSilane-POSS™ (POSS1) and Tris (Dimethylsilane)Cyclo-pentyl-POSS™ (POSS2) from Hybrid Plastics Company

obtained by Xiao and Feher, who copolymerized monofunctional methacryloyl-functionalized POSS with methyl methacrylate (MMA) [15]. Choi et al. used multifunctional glycidyl-POSS as nano-crosslinking agent for epoxy resins [6]. However, this POSS modification failed to improve mechanical and thermal properties. Tsuchida and coworkers applied metallocene-catalyzed copolymerization of monoolefin-functionalized POSS to prepare polyolefins with POSS side chains [16]. In accord with observations by Zheng et al. concerning the catalytic copolymerization of 1-olefins with norbornene-functionalized POSS, at low POSS content below 10 wt.% only marginal improvements of polyolefin polymer properties of the POSS polyolefin nanocomposites were detected [17].

In contrast to the covalent attachment of functionalized POSS, much less is known about the nanostructure formation via self-assembly of POSS which cannot form covalent bonds with the polymer backbone. For example, Li et al. incorporated $(i\text{-butyl})_8$-POSS into the vinylester polymer matrix [18]. The composite showed very large macroscopically aggregated particles of up to 300 μm. With respect to the neat vinylester no improvement of thermal and mechanical properties was visible. Blanski et al. investigated the influence of different POSS on the morphology of polystyrene composites [19]. As a function of the POSS molecular architectures, transmission electron microscopy (TEM) micrographs showed various architectures ranging from very large crystallites to molecular dispersed polysilsesquioxane molecules.

The objective of this research was to examine nanostructure formation via self-assembly of non-reactive POSS such as $[Si_8O_{12}(OSiMe_2H)_8]$ (POSS1) and $[Si_7O_9(cyclohexyl)_7(OSiMe_2H)_3]$ (POSS2), both of which are displayed in Scheme 2, during the free radical MMA bulk polymerization. The influence of POSS self-assembly and superstructure formation on the thermal, mechanical and morphological properties of the resulting PMMA-nanocomposites were investigated. Ion beam analysis (Rutherford backscattering, RBS) was used to examine surface gradient formation via POSS self-assembly and POSS accumulation at the PMMA nanocomposite surface.

Experimental

Materials

Methylmethacrylate (Fluka) was distilled under reduced pressure and stored over 3 Å molecular sieve. The free radical initiator 2,2′-azoisobutyronitrile (AIBN) was used as obtained from Fluka. The silsesquioxanes OctaSilane-POSS™ (POSS1) and Tris(Dimethylsilane)Cyclopentyl-POSS™ (POSS2), displayed in Scheme 2, were supplied by Hybrid Plastics, Fountain Valley, CA, USA.

Preparation of PMMA/silsesquioxane-nanocomposites

Methyl methacrylate (28.5 g) was degassed at room temperature at 100 mbar and then the initiator AIBN (85.5 mg, 0.3 wt.% based on MMA) was dissolved. OctaSilane-POSS™ (POSS1) and Tris(Dimethylsilane)Cyclopentyl-POSS™ (POSS2) (1.5 g, 5,3 wt.% based on MMA), respectively, were added. The mixture was stirred for 15 min using a magnetic stirrer. The resulting clear solution in case of POSS1 and the opaque solution in case of POSS2 were degassed at room temperature at 100 mbar. The mixtures were polymerized between two PTFE-coated glass plates for 48 h at 60 °C in a water bath.

Characterization and methods

The thermal behaviour was analysed by differential scanning calorimetry (DSC) using a Netzsch DSC 200. The heating rate was 10 °C/min. The thermal gravimetric analysis (TGA) was carried out using a STA 409 Thermogravimetric Analyzer from Netzsch. Samples were heated up to 600 °C with a heating rate of 10 °C/min in nitrogen flow.

Test specimens were milled by means of a Diadrive 2000 (Mutronic, Rieden, Germany). Tensile tests were conducted using a Zwick tensiometer Z005 (ISO/DP527). K_{Ic} tests were carried out by measuring the maximal force at break of compact tension specimens [20]. The data were taken at room temperature after drying the specimens at 60 °C overnight.

Morphology was examined by TEM. For TEM measurements, ultra thin sections were prepared with an Ultracut E, Reichert & Jung, ultramicrotome using a diamond knife. TEM-measurements were carried out on a LEO 912 Omega with an acceleration voltage of 120 keV.

Surface enrichment analysis was done using ion beam analysis with the RBS technique. The experiments were performed at the 7.5 MV CN Van de Graaff laboratory [21] with a beam of ^{4}He-ions with an energy of 2.3 MeV. The analyzed areas were of the size of less than 0.5 mm^2. The backscattered He-ions were detected using a Si particle detector positioned at an angle of 165° with respect to the incoming beam direction. In order to reduce kinematical broadening the detector was collimated to about 3° in the scattering plane.

Scratch resistancy tests were carried out by a scanning scratch tester SST 110 from Shimazu. The test specimens were scratched by an oscillating diamond indenter (tip radius:100 μm; scratch speed:20 μm/s), which is set down on the sample with a down speed of 1 μm/s. The covered distance is measured to the point a critical amplitude is reached. The distance to critical force is equated with the scratch resistancy.

Results and discussion

The free radical polymerization of MMA was performed in bulk at 60 °C in the presence of 5.3 wt.% POSS1 and POSS2. The PMMA and PMMA/POSS properties are listed in Table 1.

The analysis of thermal properties by means of DSC revealed significant increases of glass temperatures of the PMMA/POSS nanocomposites. In comparison to the glass temperature of pure PMMA, glass temperature increases of 18 °C were observed for POSS1 addition and of 14 °C for POSS2 addition. According to the TGA displayed in Fig. 1 all samples exhibited 100% weight loss. This indicated that no silicates were formed upon POSS thermal treatment. According to TGA the on-set temperature observed at 5 wt.% weight loss decreased from 317 °C for pure PMMA to 243 °C for PMMA/POSS1 and 265 °C for PMMA/POSS2. Although POSS is likely to sublime at elevated temperatures and contribute marginally to the weight loss due to POSS sublimation in the absence of covalent matrix attachment, this thermal stability loss encountered above 300 °C was quite unexpected.

Table 1 Properties of PMMA and PMMA/POSS nanocomposites

Properties	PMMA	PMMA/POSS1	PMMA/POSS2
Glass temperature (°C)	89	107	103
TGA total weight loss [%]	100	100	100
TGA on-set temperature at 5% weight loss	317	243	265
Young's modulus [MPa]	2560 ± 50	2350 ± 160	2340 ± 140
Stress intensity factor K_{Ic} [MNm$^{-3/2}$]	1.52 ± 0.08	1.80 ± 0.01	1.80 ± 0.05
Scratch resistance [μm]			
after H_2O treatment	2000 ± 15	2040 ± 40	2020 ± 40
after aq. NaOH treatment	1980 ± 20	1960 ± 45	1970 ± 10

The tensile testing of the PMMA/POSS nanocomposites showed that the POSS addition afforded improvements of toughness without affecting the PMMA stiffness. The Young's modulus was measured

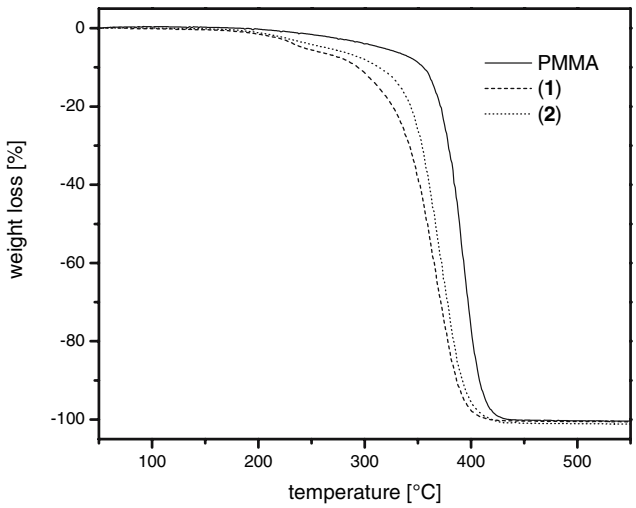

Fig. 1 Thermal gravimetric analysis of the PMMA/silsesquioxane composites

to be 2560 MPa for pure PMMA, 2350 MPa for PMMA/POSS1 and 2340 MPa for PMMA/POSS2. In contrast, toughness, as expressed by the critical stress intensity factor, increased markedly from 1.52 $MNm^{-3/2}$ for PMMA to 1.80 $MNm^{-3/2}$ for both PMMA/POSS. This 18% toughness enhancement is likely to be associated with multiple plastic deformations initiated by the presence of nanophase separated POSS which act as stress concentrators. This in situ POSS nanoparticle formation via POSS self-assembly was confirmed by means of TEM although further research is required to fully understand PMMA/POSS micromechanics.

According to the TEM image of a thin cut displayed in dispersed cube-like aggregates of up to 500 nm. This in situ particle formation is the result of POSS1 phase separation and self-assembly within the PMMA matrix. The bright area around the big particle in Fig 2a indicates poor interfacial adhesion and delamination of PMMA from the nanoparticle surfaces encountered during cutting of the thin section. Also much smaller cubes with average diameter of around 27 nm were detected (Fig. 2b).

Similar self-assembly superstructures consisting of cube-like non-adhering aggregates were observed for PMMA/POSS2 although the very small nanocube fraction was not formed (Fig. 3). This presence of non-adhering nanophases is likely to afford nanovoiding during straining, thus accounting for multiple plastic deformation and toughness enhancement.

The POSS phase separation can also occur at the PMMA/POSS surface to produce PMMA gradient materials. The surface accumulation and the in situ surface modification was examined by means of depth profiling using the ion beam RBS method. RBS is based on the elastic scattering of ions by the target atoms. Depending on the mass of the target atoms, the backscattered ions are detected with different energies,

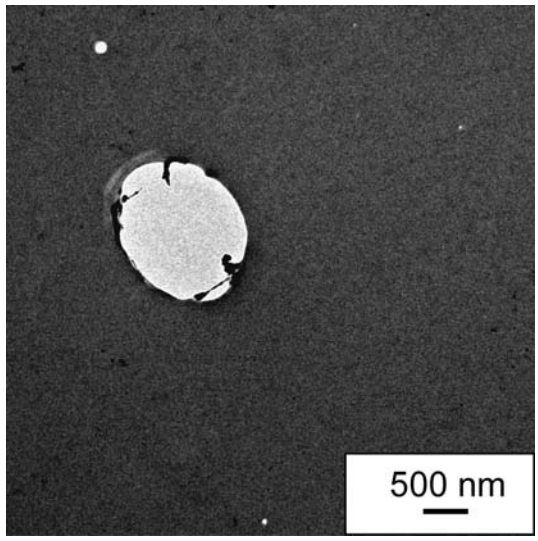

Fig. 3 TEM micrograph of PMMA/POSS2

with higher target mass meaning higher backscattered ion energy. Energy loss by incident and scattered ions provides a useful method for the measurement of depth profiles. In Fig. 4 the RBS-spectra of both sides of PMMA/POSS1 are shown. The penetration depth was determined to be about 800 nm from the surface of the sample into the material. Both energy spectra show the signals of C, O, and Si, with Si being the heaviest atom and thus resulting in the highest energy of the backscattered He-projectiles. RBS-measurements of the frontside of PMMA/POSS1 show decreasing silicon and oxygen signals with decreasing energy. This is a clear indication for the surface enrichment of POSS. The RBS measurements of the other side of PMMA/POSS1 show a rather weak decrease in the signal with decreasing energy. But an enrichment of silsesquioxane is suggested as well. The process of enrichment is

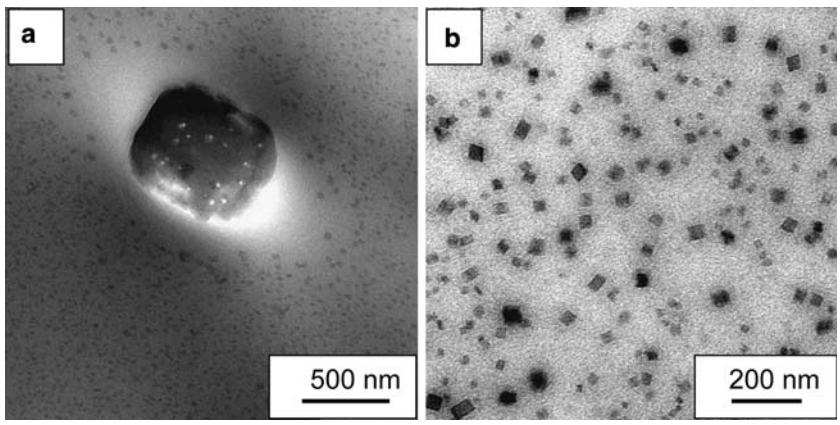

Fig. 2 TEM micrographs of PMMA/POSS1

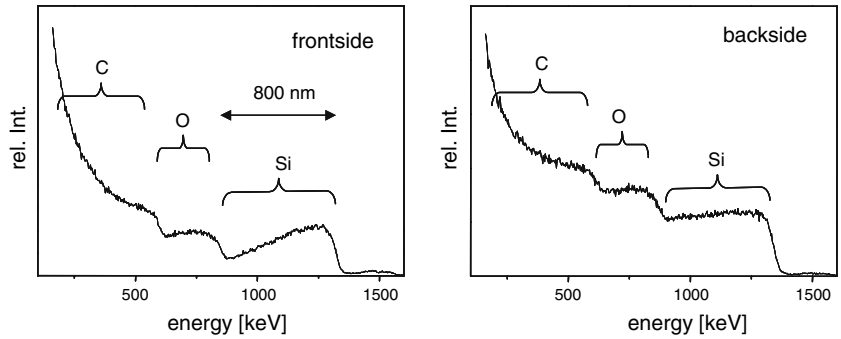

Fig. 4 ^{4}He-RBS-spectra of the frontside (left) and the backside (right) of the PMMA/POSS1 sheet

explained by diffusion of POSS 1 to the PMMA/glass interface during the polymerization driven by the lower surface energy at the PMMA/glass interface.

In Fig. 5 the RBS spectrum of PMMA/POSS2 is displayed. In this case the plateau of the Si signal shows a constant intensity with decreasing energy. In contrast to PMMA/POSS1 a homogeneous distribution of POSS2 within the PMMA matrix must be assumed. Most likely, the cyclohexyl substitution changes the POSS2/PMMA compatibility and does not favour surface migration and in situ surface gradient formation.

The in situ nanofiller surface accumulation, as evidenced by RBS measurements, offers potential for the in situ surface reinforcement via POSS self-assembly combined with POSS-mediated SiO_2 formation at the surface obtained via POSS polycondensation. Such in situ surface hardening could afford improved scratch resistance. POSS containing Si–H groups are well known to undergo polycondensation reaction, especially in alkaline media, when Si–H reacts to form hydrogen and Si–O–Si bonds which link together POSS and produce SiO_2 [22]. Therefore, PMMA/POSS nanocomposites were examined with respect to its scratch resistance as a function of water and NaOH surface treatments. Scratch resistance tests were conducted by measuring the distance to the critical force using a scanning scratch tester SST 110 from Shimazu. Each test specimen was conditioned for 10 h in distilled water or 1 M NaOH-solution. Table 1 lists the experimental results concerning the scratch resistance. At 5, 3 wt.% POSS content there is no indication for effective surface reinforcement associated with improved scratch resistance.

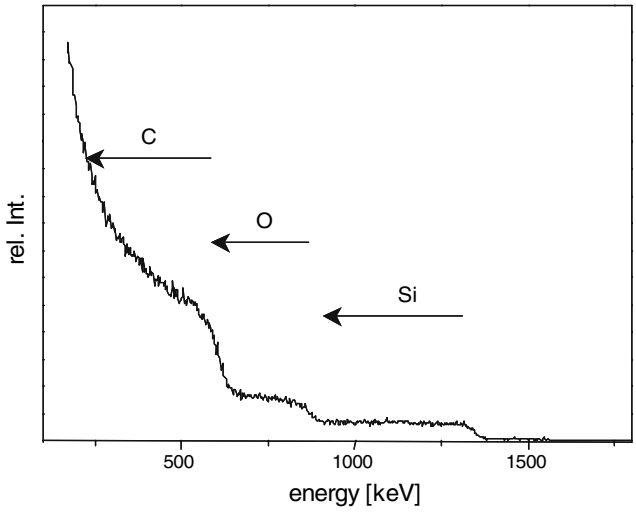

Fig. 5 ^{4}He RBS spectra of PMMA/POSS2

Conclusion

POSS1 and POSS2 dissolve in MMA and phase separate during MMA polymerization to produce PMMA/POSS nanocomposites. The POSS phase separation combined with the POSS self-assembly represents the key to the in situ formation of uniformly dispersed cube-like nanoparticles with average diameters varying between 20 nm and 500 nm. No dispersion and handling problems typical for dispersing conventional nanofillers were encountered in this POSS mediated in situ nanofiller forming process. In the absence of covalent bond formations between POSS and PMMA, non-adhering cube-like nanoparticles were formed. Such non-adhering nanocubes represent novel PMMA toughening agents which improve PMMA toughness without affecting stiffness, as evidenced by an 18% increase of the stress intensity factor K_{Ic}. According to the surface depth profiling by means of RBS POSS1 accumulated at the PMMA surface to produce PMMA gradient materials. At 5, 3 wt.% POSS1 content neither bulk nor surface reinforcement were achieved. Further fine tuning of the POSS molecular architectures, especially with respect to POSS polycondensation, is required to improve the performance of in situ formed non-adhering nanofillers and promote the in situ formation of functional nanocoatings.

Acknowledgement The authors gratefully acknowledge the financial support of their research by the Deutsche Forschungsgemeinschaft and SFB 428.

References

1. LeBaron PC, Wang Z, Pinnavaia T (1999) J Appl Clay Sci 15:11
2. Okada A, Kojima Y, Kawasumi M, Fukushima Y, Kurauchi T, Kamigaito O (1993) J Mater Res 8:1179
3. Akelah A, Salahuddin N, Hiltner A, Baer E, Moet A (1994) Nanostruct Mater 4:965
4. Giannelis EP (1996) Adv Mater 8:29
5. Zilg C, Thomann R, Baumert M, Finter J, Mülhaupt R (2000) Macromol Rapid Commun 21:1214
6. Choi J, Harcup J, Yee AF, Zhu Q, Laine RM (2001) J Am Chem Soc 123:11420
7. Schwab JJ, Lichtenhan JD (1998) Appl Organometal Chem 12:707
8. Haddad T, Viers BD, Philips SH (2001) J Inorg Organomet Polym 11:155
9. Zhang W, Fu BX, Seo Y, Schrag E, Hsiao B, Mather PT, Yang, N-l, Xu D, Ade H, Rafailovich M, Sokolov J (2002) Macromolecules 35:8029
10. Zhang C, Laine RM (2000) J Am Chem Soc 122:6979
11. Zheng L, Kasi RM, Farris RJ, Coughlin EB (2002) J Polym Sci, Part A: Polym Chem 40:885
12. Zhang C, Babonneau F, Bonhomme C, Laine RM, Soles, Cl, Hristov HA, Yee AF (1998) J Am Chem Soc 120:8380
13. Neumann D, Fisher M, Tran L, Matisons JG (2002) J Am Chem Soc 124:13998
14. Baney RH, Itoh M, Sakakibara A, Suzuki T (1995) Chem Rev 95:1409
15. Xiao J, Feher FJ (2002) Polym Prepr 43:504
16. Tsuchida A, Bolln C, Sernetz FG, Frey H, Mülhaupt R (1997) Macromolecules 30:2818
17. Zheng L, Farris RJ, Coughlin EB (2001) Macromolecules 34:8034
18. Li GZ, Wang L, Toghiani H, Daulton TL, Pittman Jr CU (2002) Polymer 43:4167
19. Blanski RL, Philips SH, Chaffee K, Lichtenhan J, Lee A, Geng HP (2000) Polym Prepr 41:585
20. Knott JF (1973) Fundamentals of fracture mechanics. Butterworths, London
21. Brenn R, Haug C, Klar U, Zander S, Alt KW, Jamieson DN, Lee KK, Schutkowski H (1999) Nucl Inst Meth B 158:582
22. Baines JE, Eaborn C (1955) J Am Chem Soc 4023